Unravelling Work Function Contributions and their Engineering in 2H-MoS$_2$ Single Crystal Discovered by Molecular Probe Interaction

Amir Ghiami, [†,#,Δ] *Melanie Timpel,* [‡, Δ,] * *Marco V. Nardi,* [#, ‡,] * *Andrea Chiappini,* [§] *Petr Nozar,* [Δ] *Alberto Quaranta,* [‡] *and Roberto Verucchi* [#]

[†]Department of Chemistry, Life Science and Environmental Sustainability - University of Parma, Parco Area delle Scienze 17/A, 43124 Parma, Italy

[#]IMEM-CNR, Institute of Materials for Electronic and Magnetism, Trento unit c/o Fondazione Bruno Kessler, Via alla Cascata 56/C, Povo, 38123 Trento, Italy

[‡]Department of Industrial Engineering, University of Trento, Via Sommarive 9, 38123 Trento, Italy

[§]CNR-IFN, CSMFO Lab, Via Alla Cascata 56/C, 38123 Trento, Italy

ABSTRACT. In this study, a comprehensive investigation of the role of sulfur vacancies on the electronic structure and surface reactivity of molybdenum disulfide is presented. A 2H-MoS$_2$ single crystal was annealed at two different temperatures, namely 300 and 500 °C in vacuum, in order to generate sulfur vacancies in a controlled manner. The detailed characterisation of the electronic structure by means of X-ray and ultra-violet photoelectron spectroscopy clearly evidences the formation of a strong surface dipole as well as surface band bending due to the excess of negative charge on the Mo centers, as a consequence of the generated sulfur vacancies. After thermal treatment, a mercaptoundecylphosphonic acid molecule, which consists of a thiol (S-H) tail group and a phosphonic acid group on the other end, was covalently attached on the surface through wet chemical functionalization in order to refill the sulfur vacancies. As a consequence of the vacancy refilling, the surface band bending is reversed and the surface dipole is remarkably decreased being close to the initial value of the pristine surface.

1. INTRODUCTION

Transition metal dichalcogenides (TMDCs) are a group of materials that have attracted a great attention due to their outstanding electronic, optical, chemical and physical properties.[1,2] Within the TMDCs, molybdenum disulfide (MoS$_2$) consists of individual sandwiched S-Mo-S layers assembled by weak van der Waals (vdW) interaction. The coordination of the Mo atom in layered MoS$_2$ is mostly found to be either trigonal prismatic (2H polymorphs) or octahedral (1T polymorphs). 2H-MoS$_2$ is found to be semiconducting with an indirect band gap of 1.2 eV in the bulk form that change to a direct band gap of 1.9 eV when it is present as monolayer, whereas its 1T- MoS$_2$ shows metallic behavior. The tunable band gap, the good light-conversion efficiency and charge mobility together with piezoelectric properties[3] leads the MoS$_2$ to be a promising

candidate for several applications spanning from sensors, transducers, energy conversion and electronics.

To fully harness the potential of MoS_2 and widen its application prospect, different studies concerning surface reactivity and chemical composition were done. In this scenario, sulfur vacancies which are the most abundant defects located on the surface or edges of the material[4,5] play a crucial role since they are found to be chemically more reactive[5] than the perfect lattice and they have the tendency to react with molecules to form strong bonds.[4] This fact originates from the formation of unpaired electrons present along the edges and lattice defects of MoS_2.[6] Regardless if flakes, 2D or few-layered MoS_2 are prepared, the presence of different types of sulfur vacancies such as mono, double, tri, (multi-) line and/or clusters are present.[7–10]

In many studies[6,11–16] the potential of sulfur defects have been exploited to functionalize MoS_2 with a variety of molecules containing thiol as anchoring group. However, a deep investigation of the role of sulfur vacancies and surface stoichiometry on the electronic structure of 2H-MoS_2 and its implication on the surface reactivity and functionalization has not yet been reported. Recently performed density functional theory (DFT) calculations[17] predicted that thiol-derived molecules with electron-donating moieties promote a sulfur vacancy repairing reaction, whereas electron-withdrawing groups facilitate the surface functionalization of MoS_2. *Nguyen et al.*[18] functionalized MoS_2 with a variety of organic thiols with different electron-withdrawing capabilities, for tuning the electronic levels of MoS_2 flakes, which could pave the way for producing more efficient electronic and light emitting devices as well as solar cells.[19] Based on the above-mentioned studies, a more detailed knowledge of the phenomena that lead to the generation of superficial dipoles, surface charge redistribution and work function change with respect to the amount of surface defects and functionalizing molecules, becomes of fundamental importance.

To maximize the benefit from molecular functionalization, the coverage can be improved with a high density of anchoring sites promoting the chemical reactivity. Since the sulfur vacancies present on the edge and the basal plane of MoS_2 are found to be the active sites for the thiol group, it can be inferred that the functionalization efficiency depends on the amount of sulfur vacancies present on the edge and basal plane of MoS_2.[15] In the case of MoS_2 nanoflakes derived by chemical or mechanical exfoliation, due to the harsh nature of the processes, the yielded product is highly defective and suitable for efficient functionalization processes.[20] A remarkable functionalization efficiency has been achieved, in particular due to the high number of edge defects present on the flakes.[4,14,21] However, this is not the case for large-area MoS_2 layers, which can be obtained by chemical vapor deposition (CVD), pulsed laser deposition (PLD) or other scalable synthesis techniques, since the edges play a minor role and the material properties are dominated by the basal plane.

In order to achieve an efficient functionalization and to produce hybrid systems for high-performance devices in which the organic/inorganic interface processes play a main role, we investigated the change of both electronic structure and reactivity of highly stable $2H\text{-}MoS_2$ single crystal after thermal annealing inducing sulfur defects. The energy level tuning of $2H\text{-}MoS_2$ via surface treatment and its effect on surface reactivity was deeply investigated.

2. EXPERIMENTAL SECTION

Samples. Thermal treatment and surface functionalization were carried out on MoS_2 bulk single crystals (SPI Supplies, purity > 99.9 %). As-received crystals were sonicated in trichloroethylene, acetone and 2-propanol consequently for 10 minutes in each solvent, and finally dried with a nitrogen gas flux. Figure S1 (Supporting Information) shows the C 1s, O 1s and N 1s core levels of an as-reveived crystal and after solvent-cleaning (and blowing dry with

nitrogen), proving that in both cases neither carbon, oxygen nor nitrogen were present on the pristine MoS_2 single crystals.

Thermal treatment. To perform thermal treatment, an ultra-high vacuum chamber with a working pressure of $\sim 4\times10^{-10}$ mbar was used. The samples were heated at 300 and 500 °C, respectively, each for 1h. In the following, the thermally treated samples are denoted as TT300 and TT500.

X-ray photoelectron spectroscopy. After thermal treatment, XPS and UPS analyses were performed *in-situ* (i.e., in the same UHV chamber without breaking the vacuum to avoid any gas adsorption on the freshly annealed surface) with a non-monochromatized Mg Kα X-ray source (emission line at 1253.6 eV) and a helium discharge lamp (emission line at 21.21 eV). A VSW HA 100 electron analyzer was used to analyze the energy of the emitted photoelectrons.[22] The total resolution was 0.8 eV for XPS and 0.10 eV for UPS analysis. The binding energy (BE) scale of XPS spectra was calibrated by using the Au 4f peak at 84.0 eV as a reference, while UPS BEs were referred to the Fermi level of the same Au clean substrate. The MoS_2 single crystal and the clean Au substrate were mounted on the same sample holder and connected to the same electrical ground. Core level analyses were performed by Voigt line-shape deconvolution after background subtraction of a Shirley function. UPS analyses were performed with the samples biased at -7 V to compensate the analyzer work function.

Surface functionalization. A wet-chemical method was used to functionalize the (untreated) pristine and TT500 sample. The samples were immersed into a 1mM ethanol solution of 11-mercaptoundecylphosphonic acid (MUPA, purchased from Sigma Aldrich) and kept for 24 hours. Thermally treated samples were extracted from UHV and immediately immersed into the solution to minimize gas adsorption on the MoS_2 surface from the atmosphere. Before inserting

the functionalized samples into the analyzing chamber, they were sonicated for 5 min in ethanol to remove weakly bound molecules and dried with nitrogen. Figure S2 (Supporting Information) shows the C 1s and O 1s core levels of MUPA after functionalization of the thermally treated MoS_2 surface (TT500).

Raman spectroscopy. Non-resonant Raman spectra were acquired at room temperature using a LabRAM Aramis (Horiba Jobin-Yvon) which is equipped with a diode-pumped solid-state laser line of 532 nm. The laser line was focused on the sample by a 100× microscope objective lens. The collected light was dispersed by an 1800 grooves/mm spectrometer and detected by a charge-coupled device (CCD) detector. The Rayleigh line below 100 cm^{-1} was filtered. The silicon Raman band which is located at 520 cm^{-1} was used as reference. The resolution of the spectra obtained was 1 cm^{-1}.

FT-IR spectroscopy. The FT-IR spectra of the pristine and functionalized MoS_2 samples were obtained using a Bio-Rad model FTS-165 instrument. The analysis was performed in an attenuated total reflectance (ATR) mode on diamond single reflection, in the frequency range of 400- 500 cm^{-1}.

3. RESULTS AND DISCUSSION

Thermal Treatment. The Mo 3d and S 2p core levels of pristine and thermally treated MoS_2 single crystals are shown in Figure 1a and b, respectively. The values of the energy shifts of the thermally treated samples with respect to the pristine one and the relative stoichiometry are summarized in Table 1. The peak corresponding to the Mo3d$_{5/2}$ core level of the pristine sample was found at a binding energy (BE) of 229.55 eV, whereas the S 2p peak was found at 162.36 eV, in agreement with previous reports.[23,24] The stoichiometry, evaluated by the ratio between the S

2p/Mo 3d peak areas was found to be 1.92 for the pristine $2H\text{-}MoS_2$ and decreases to 1.86 and 1.72 for the TT300 and TT500 sample, respectively. After annealing, a shift to lower BEs, increasing with the treatment temperature, occurs for both core levels, which is in agreement with previous findings.[25]
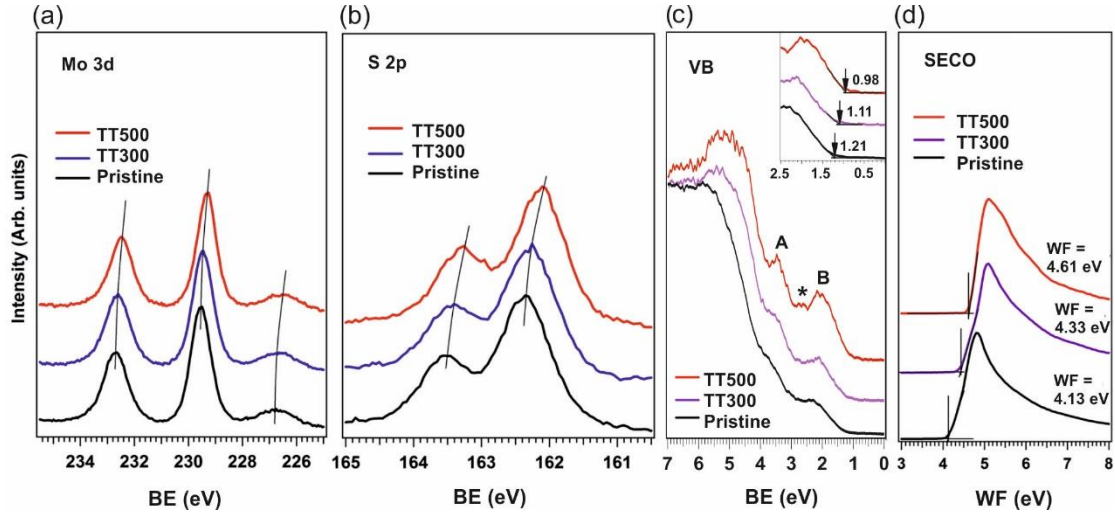
Figure 1. (a) Mo 3d and (b) S 2p core level spectra of pristine and thermally treated (TT300 and TT500) MoS_2 single crystals. (c) Corresponding valence band (VB) region UPS and (d) SECO spectra. The inset in (c) shows zooms into the near E_F region.

Table 1. Binding energy (BE), valence band maximum (VBM), work function (WF) values and corresponding changes in pristine and thermally treated samples.

	Mo 3d$_{5/2}$ $(\Delta\,BE)^{a)}$	S 2p $(\Delta\,BE)^{a)}$	VBM $(\Delta\,BE)^{a)}$	WF $(\Delta\,WF)$	S / Mo [2.0]
Pristine	229.55	162.36	1.21	4.13	1.92
TT300	229.45	162.26	1.11	4.33	1.86
	(- 0.10)	(- 0.10)	(- 0.10)	(+ 0.20)	

TT500	229.30	162.11	0.98	4.61	1.72
	(- 0.25)	(- 0.25)	(- 0.23)	(+ 0.48)	

[a)]BE, (Δ BE) and (Δ WF) are expressed in [eV];

According to previous studies,[26,27] downward shifts of the core levels are attributed to the excess of negative charge on the surface. This effect can be related to the removal of sulfur from the surface, leaving behind excess of molybdenum atoms with electron lone pairs (see schematically in **Figure 2**a), as also evidenced by the change in the S 2p/Mo 3d ratio. Thus, the surface is enriched with negatively charged sulfur vacancies.[28] This makes the surface locally more negative; however, the surface remains globally neutral and not in an anionic state. Moreover, since sulfur vacancies have the lowest formation energy among all the possible defects in the MoS_2 lattice,[29] they are expected to be the most abundant defects on the surface after thermal treatment.

The line shape of the core levels remains almost unchanged and the value of the energy shift is found to be the same for both core levels, suggesting that no important change in the chemical state took place with the annealing. In Figure 1c the valence band maximum (VBM) of the thermally treated samples is found at lower BEs, in agreement with the core level shifts. The VBM shift for both samples TT300 and TT500 is equal to the shift in the corresponding Mo 3d and S 2p core levels.

Besides VBM shifts, we observed that the two major states at around 3.8 and 2.4 eV (labeled as A and B in Figure 1c) appeared more prominent after annealing at 300 °C. By further increasing the temperature up to 500 °C, another state located between the two latter ones appeared at around 3.0 eV (labeled as * in Figure 1c) related to new defect-induced electronic states, as already reported in some studies based on density functional methods.[30,31]

In Figure 1(d), the corresponding secondary electron cutoff (SECO) spectra of the samples is reported. Thermal treatment and the consequent formation of sulfur vacancies on the MoS₂ surface leads to an increase in the work function highlighting a p-type behavior[32,33] of the thermally treated MoS₂ surface, differently from the bulk MoS₂ that is naturally showing n-type character. It is noteworthy that any gas adsorption (such as oxygen/water and/or nitrogen) at S vacancies that has been previously shown to induce p-type doping[34,35] can be ruled out, since pristine samples showed no detectable contaminations (see Figure S1, Supporting Information), and both annealing and analysis were performed in the same UHV chamber. Furthermore, the increase of the work function is higher than the shifts observed for core levels and valence band, pointing to an overlap of two different surface processes. Their origin can be understood by considering the chemical environment of an individual sulfur vacancy as shown in Figure 2a.
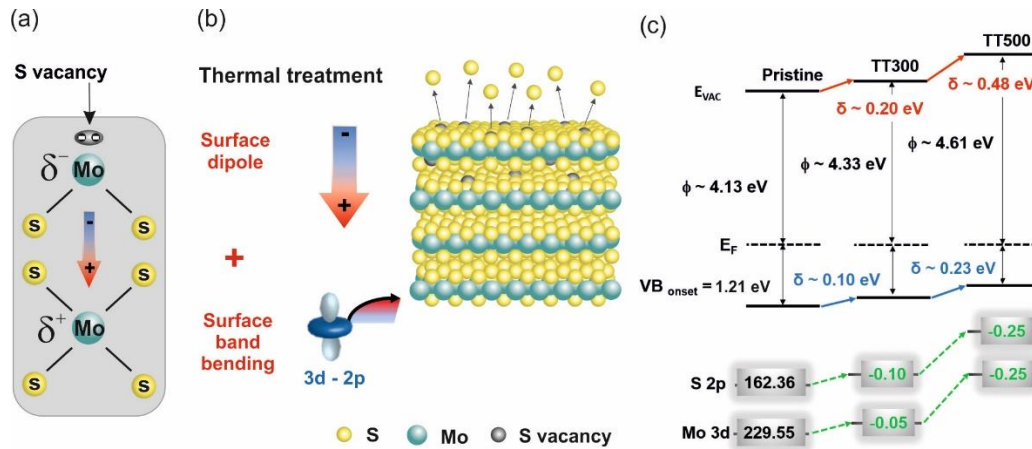
Figure 2. (a) Schematic illustration of the chemical environment of an individual sulfur vacancy; (b) the removal of sulfur atoms from the MoS₂ surface by UHV thermal treatment leads to the formation of a surface dipole and band bending; (c) energy level diagram of pristine and thermally treated samples.

After S removal, an excess of negative charge (δ^-) is generated by the electron lone pair localized on the topmost Mo center with respect to the Mo center in the next MoS_2 layer (δ^+). Even though there might be some interlayer charge compensation due to the repulsive Coulombic interaction in the topmost vacancy-rich MoS_2 layer, the absence of covalent bonds between the different MoS_2 layers (only vdW forces) will not allow for full charge compensation, leading behind a net excess of negative charge localized on the topmost MoS_2 layer. Hence, modification of the surface occurred due to the introduction of surface defects by annealing the bulk single crystal MoS_2 so that the electrostatic field close to the surface changes. To account for the modified electrostatic field, we assume an electrostatic model previously developed to elucidate work function changes due to molecule adsorption,[36] where the total change of the work function ($\Delta\phi_{tot}$) can be determined by the sum of independent contributions.

In the present study, we attribute the total change of the work function ($\Delta\phi_{tot}$) after thermal treatment to the formation of an interface dipole $\Delta\mathbf{V}_{int.dip}$ (due to net excess of negative charge localized on the topmost MoS_2 layer), in analogy to the adsorption of electron acceptor/donor molecules on semiconducting surfaces,[37,38] where net charge transfer between donor/acceptor and substrate occurs. This interface dipole can be typically divided into a surface band bending ($\Delta\phi_{BB}$) contribution and the formation of a surface dipole moment ($\Delta\phi_{SD}$):

$$\Delta\phi_{tot} = \Delta V_{int.dip} = \Delta\phi_{BB} + \Delta\phi_{SD} \tag{1}$$

For the samples TT300 and TT500, the downward shift observed for core levels is 0.10 and 0.25 eV (see Table 1), which is assumed to be equal to the surface band bending and is partially responsible for the work function increase of each sample. It has already been found that surface

defects are one of the principal reasons for surface band bending.[25,39] In addition, the formation of a net dipole pointing towards the bulk implies an increase of the sample work function.[40–42] Therefore, we attribute the other part of the work function increase (0.10 and 0.23 eV, respectively) to the formation of a surface dipole moment. The simple model in Figure 2b summarizes the fact that both the formation of a surface dipole and surface band bending contribute to the increase of the work function and hence p-type behavior of thermally treated MoS_2. Figure 2c schematically shows the interfacial energy-level diagram of pristine and thermally treated MoS_2 surfaces, as derived from our UPS measurements.

In order to estimate the defects on the surface created by thermal treatment, the Mo 3d core levels were fitted (Figure 3(a)). It was found that the Mo 3d line shape cannot be fitted by a single Mo 3d doublet, unless another doublet located 0.3 - 0.4 eV below the main doublet is added. The main doublet (in the following denoted by Mo_{MoS_2}) corresponds to the six coordinated molybdenum atoms that are located at the center of the trigonal prismatic crystal structure of 2H-MoS_2. The second doublet denoted by Mo_v is attributed to unsaturated molybdenum atoms, which are present in the thermally treated samples mainly due to sulfur removal. Sulfur vacancies are also present in the pristine sample in a low amount which arises from intrinsic defects in the as-received crystals.[39] The appearance of the second doublet in Mo 3d spectra has already been reported in some other works.[26,27,43,44] By annealing the sample up to 500 °C, the full width at half maximum (FWHM) of the Mo_{MoS_2} peak increased from 0.85 eV to 0.91 eV, which is a clear indication for the appearance of defects and disorders in the crystal structure.[27]
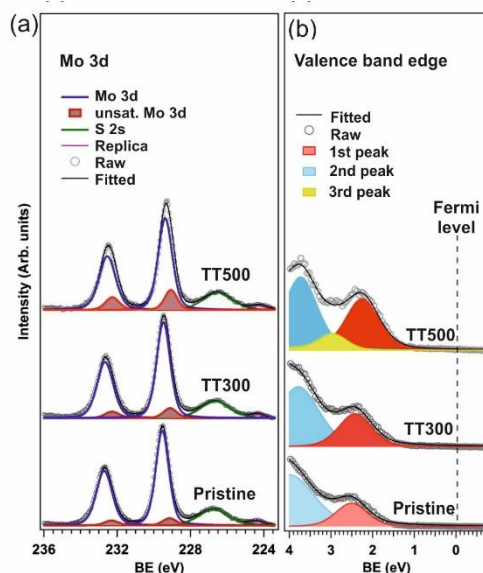
Figure 3. (a) Fitted Mo 3d - S 2s core levels, and (b) fitted valence band of pristine and thermally treated (TT = 300, 500°C) MoS$_2$ single crystals, showing the evolution of defect-induced states after annealing.

The areas attributed to the doublet peak corresponding to unsaturated molybdenum in pristine and thermally treated samples at 300 and 500°C are found to be (8.0 ± 0.4) %, (10.5 ± 0.5) % and (19.6 ± 1.0) % of the total area. In other words, annealing the sample at 300°C for 1 h increased the amount of defects by ~30% relative to the pristine sample; this value becomes ~143% for the sample annealed at 500°C. It is important to note that the obtained values do not represent the absolute amount of surface defects, but are an estimation of their relative increase induced by annealing.

Assuming that the relative increase of the structure in the valence band edge states are attributable to the higher amount of sulfur vacancies;[45,46] an increase of ~33% and ~139% in the area of the valence band edge states for the samples TT300 and TT500 is found (see Figure 3b). These values are in agreement with the estimation of defect-induced states via XPS.

Surface Functionalization. Surface functionalization with an alkanethiol (MUPA) was used to investigate the effect of sulfur vacancy compensation via a thiol anchoring group on the electronic structure of MoS_2. In particular, the functionalization was performed on pristine and thermally treated $2H$-MoS_2 samples and the change in the surface dipole and surface band bending was investigated. It is expected that the thiol group (-SH) will react with a sulfur vacancy and the electron-withdrawing end group (i.e., phosphonic acid) facilitates functionalization with the functionalizing molecule attached to the surface, over a local sulfur vacancy substitution, where only the S^{2-} generated from the thiol group is covalently bound to Mo centers.[17] Independent on the structure of the S vacancies present on the sample, e.g., mono, double, line or clusters,[7–10] the chemical reactivity with a thiol group will be similar[47] and they can strongly bind the MUPA molecule. Furthermore, MUPA was chosen due to its negligible intrinsic dipole moment. Thus, any changes on the MoS_2 electronic structure can be mainly referred to binding effects. Besides this, the phosphonic acid end group provides a molecule fingerprint in the XPS spectra to evaluate the functionalization efficiency. Figure 4a shows the P 2p core levels of the untreated pristine sample (i.e., neither thermal treatment nor functionalization) and two functionalized samples, namely functionalized pristine (without thermal treatment) and functionalized thermally treated (TT500) sample. Whereas the P 2p core level region of the untreated pristine sample reveals a negligible phosphorus signal, the two functionalized samples exhibit a detectable P 2p peak stemming from the molecule. As can be seen, the intensity of the P 2p core level is higher for the functionalized + thermally treated sample than for the only functionalized pristine one, which is a clear indication of a higher number of molecules present on the thermally treated sample.
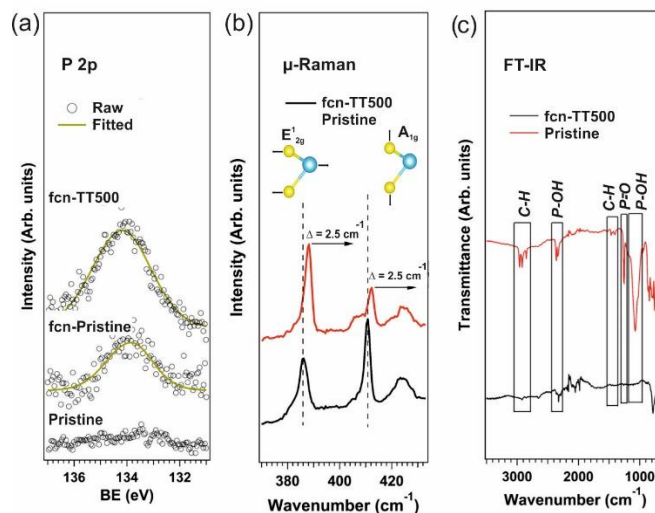
Figure 4. (a) P 2p core level of untreated pristine, functionalized pristine (fcn-pristine) and functionalized thermally treated (fcn-TT500) MoS_2 single crystal. (b) μ-Raman and (c) FT-IR spectra of pristine and functionalized (TT500) MoS_2 single crystal.

To further prove the presence of intact molecules on the surface, μ-Raman and FT-IR measurements were performed on the pristine and functionalized TT500 sample, see Figure 4b and c. The Raman spectra (Figure 4(b)) show the typical E_{2g}^1 and A_{1g} vibrational modes which arise from in-plane opposite vibration of two sulfur atoms with respect to molybdenum and out-of-plane vibration of two sulfur atoms in opposite direction, respectively. Due to functionalization and the consequent interaction at the interface of molecule/substrate, a shift toward higher wavenumbers occurs in the Raman peaks. Such an upward shift of the MoS_2 characteristic Raman peaks due to thiol treatment has already been reported by Cho et al.[13] The FT-IR spectrum obtained from functionalized MoS_2 (Figure 4(c)) is mainly dominated by the components of the phosphonic acid and the carbon chain of the molecule, which confirms the presence of MUPA molecules on the surface. Since the samples were sonicated after the functionalization process to remove any unbounded molecules, we assume that all the molecules detected on the surface strongly interact

with the MoS_2 substrate. The typical C 1s and O 1s core level spectra of the intact MUPA molecule chemisorbed on the thermally treated MoS_2 surface (TT500) are shown in Figure S2 (Supporting Information).

Figure 5 a-c shows the Mo 3d and S 2p core levels, and SECO spectra of the functionalized TT500 sample (fcn-TT500) in comparison with the untreated pristine and TT500 sample. After attaching the MUPA molecule, the Mo 3d and S 2p core levels exhibit the same BE positions than the pristine $2H$-MoS_2. In addition, the work function is decreased and almost reaches its initial value (see Figure 5(c)). The backward shift of the core levels is an indication of complete passivation of the defects through filling the sulfur vacancies at the surface by the thiol group of the molecule. Hence, the surface charge is partially neutralized and the corresponding surface dipole is much smaller than in the thermally treated sample (see Figure 5d). Furthermore, band bending effects are reversed, pointing to an almost complete compensation of the electric field at the surface. Such a backward shift of the Mo 3d and S 2p core levels implies a strong interaction between the molecule and the substrate suggesting an effective filling of the surface vacancies. The change of the electronic structure of $2H$-MoS_2 after functionalization (i.e. sample fcn-TT500), leading to an almost complete recover of the initial $2H$-MoS_2 electronic structure is summarized in the energy level diagram reported in Figure 5(e), the values are reported in Table 2.
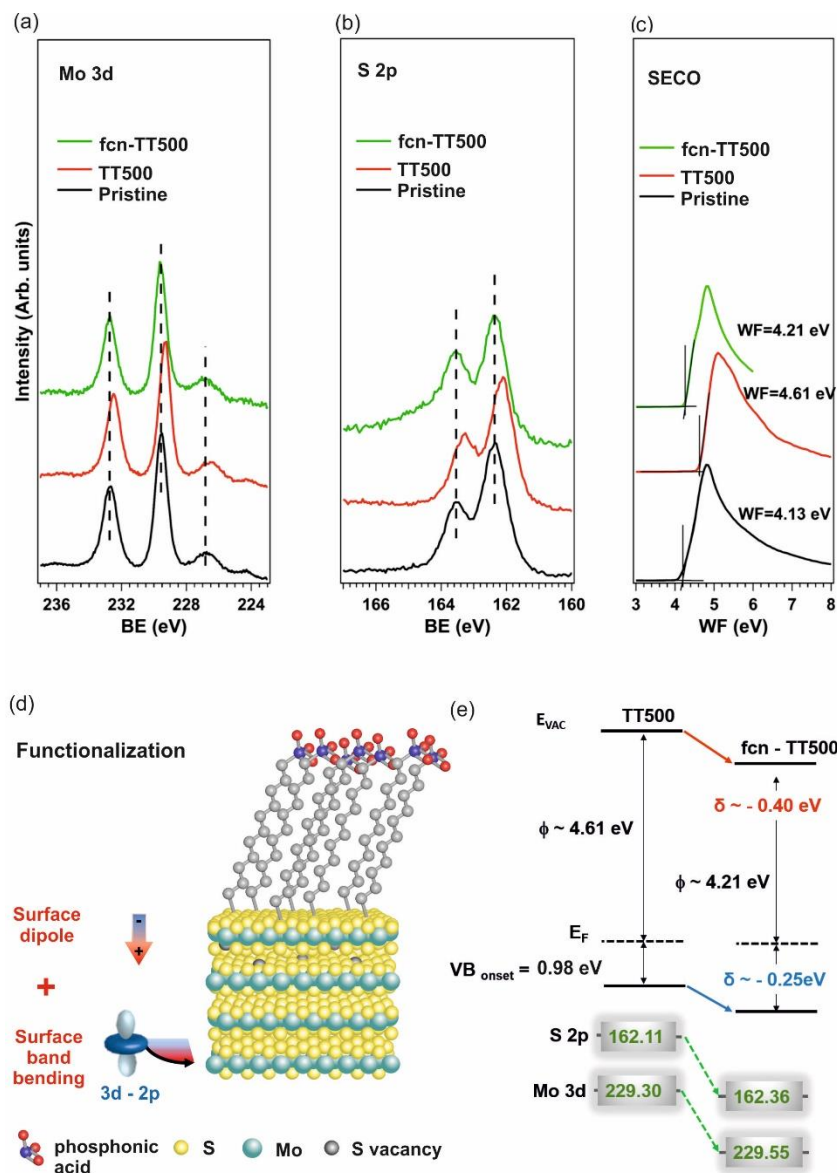
Figure 5. (a) Mo 3d, (b) S 2p core levels and (c) SECO of functionalized (fcn) sample after thermal treatment (TT = 500°C) in comparison with pristine sample and thermal treatment only. (d) Schematic illustration of the functionalization of thermally treated MoS$_2$. (e) Energy level diagram of thermally treated and functionalized samples.

Table 2. Binding energy (BE), valence band maximum (VBM), work function (WF) and S/Mo ratio changes after functionalization by MUPA.

	Mo 3d$_{5/2}$	S 2p	VBM	WF	S / Mo
	(Δ BE)[a]	(Δ BE)[a]	(Δ BE)[a]	(Δ WF)	[2.0]
TT500	229.30	162.11	0.98	4.61	1.72
fcn-T500	229.55	162.36	1.21	4.21	1.89
	(+ 0.25)	(+ 0.25)	(+ 0.23)	(- 0.40)	

[a]BE, (Δ BE) and (Δ WF) are expressed in [eV];

Figure 6 shows the deconvolution of the (a) Mo 3d – S 2s and (b) S 2p core levels for the functionalized pristine and functionalized TT500 sample. For the sake of comparison, the core levels of the untreated pristine sample is also reported. The Mo 3d – S2s core level region confirms the presence of a second S 2s peak (green in Figure 6a) that only appears in functionalized samples, and therefore, it is attributable to the molecule. The S 2s peak of the molecule is located at 227.97 eV, which is ~1.30 eV higher than the S 2s peak arising from the substrate. The S 2p core levels of the functionalized samples (Figure 6(b)) is comprised of two doublets that correspond to sulfur atoms of the molecule at ~164.0 eV and the 2H-MoS$_2$ substrate at ~162.35 eV. Although surface functionalization was achieved by filling sulfur vacancies with thiol groups, the S 2p BE of surface-bound (i.e., reacted) MUPA lies ~1.65 eV above the S 2p stemming from sulfur sites in 2H-MoS$_2$ environment, which is due to the presence of the long alkyl chain and phosphonic acid group in the molecule.
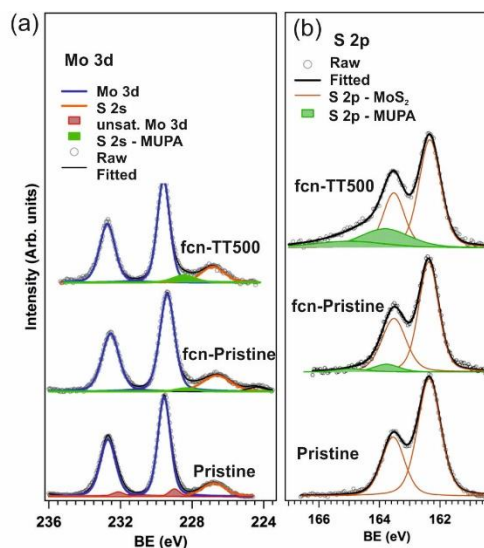
Figure 6. Fitted (a) Mo 3d - S 2s and (b) S 2p core levels of pristine, functionalized pristine and functionalized thermally treated (TT500) MoS$_2$ single crystal, showing the increase in molecule-attributed states after functionalization.

The molecular surface coverage per surface area was calculated to estimate the functionalization efficiency. The approach is based on the fact that the photoelectrons from the substrate are exponentially attenuated by the organic layer.[48] Hereafter we assume that the immersion of the samples in the molecule's solution followed by sonication yielded a monolayer of MUPA, which is uniformly distributed on the MoS$_2$ substrate. By analyzing the Mo 3d and S 2p core levels, the surface coverage of MUPA on MoS$_2$ can be estimated. Calculation of the surface coverage was done as described by Wang et al.[49] and assuming a density for the 2H-MoS$_2$ crystal and the MUPA film of 5.06 g/cm^3 and 1.4 g/cm^3, respectively. The surface coverage for the functionalized pristine and functionalized TT500 samples is found to be ~ 0.87 mol/nm^2 and ~ 2.1 mol/nm^2, respectively. According to these values, the number of molecules on the thermally treated sample is about three times higher than the number of molecules present on the untreated sample. Hence, the sulfur

defects introduced on the surface by thermal treatment facilitate the thiol molecules to be attached on the surface, which yielded a three times higher functionalization efficiency relative to the untreated functionalized substrate. Such effective functionalization for the TT500 sample leads to an almost complete clearance of the surface band bending as evidenced in Figure 5a-b by the backward shift of the substrate core level. Moreover, the almost negligible intrinsic dipole moment of the MUPA molecule, together with the compensation of the negative charge at the surface, leads to a substantial annihilation of the surface dipole that allows for an almost complete recovery of the substrate's initial work function. This process can be explained and justified by an effective compensation of charges: the excess of negative charges localized on the Mo centers, which are initially generated by the sulfur vacancies after thermal annealing, are compensated by filling the sulfur vacancies with the thiol groups of the molecule.

4. CONCLUSIONS

Since sulfur vacancies play a crucial role in determining the electronic structure of MoS_2 by changing the surface reactivity for any subsequent molecular functionalization, a fundamental study to investigate the formation of such defects and their role in the surface electronic structure was performed. For this purpose, a pristine 2H-MoS_2 single crystal was thermally treated at 300 and 500°C (in UHV), and compared with the pristine state. The amount of sulfur vacancies, as estimated via XPS, increased by about ~30 and ~140%, respectively in comparison to the vacancies natively present on pristine 2H-MoS_2. The subsequent excess of negative charge on the Mo centers at the surface leads to the formation of a surface dipole that strongly modifies the electric field at the surface allowing a WF increase of ~0.48 eV with a surface band bending of ~0.25 eV on 2H-MoS_2 thermally treated at 500°C. The possibility to fill the vacancies and

restore the original electronic structure of 2H-MoS$_2$ surface was tested by means of molecular functionalization of the thermally treated surface with a thiol-derived molecule having a phosphonic acid group at one end. The surface functionalization resulted in the formation of a homogeneous and densely packed layer of MUPA (i.e., surface density of ~ 2.1 mol/nm^2) that filled almost completely the sulfur vacancy sites generated by thermal treatment. The excess of negative charge on the Mo centers was then compensated by the thiol (-SH) groups of the molecule, bringing back the surface to the almost neutral state. Consequently, the surface band bending is completely recovered, and the Mo 3d and S 2p core levels move back to the original values as in the pristine 2H-MoS$_2$. The WF of the MUPA functionalized sample almost recovers the initial value with an offset of only 0.08 eV with respect to the pristine surface. This is attributable to a small surface dipole, related to the presence of only a few remaining sulfur vacancy sites.

The present study highlights how the surface treatment of 2H-MoS$_2$ and specifically the generation of sulfur vacancies at the surface can strongly affect the electronic structure of the first interface and consequently its reactivity. Moreover, via an efficient molecular functionalization we demonstrated how the sulfur vacancies can be filled via a thiol-derived molecule, restoring the initial properties of the 2H-MoS$_2$ surface. The rationalization of the change in the electronic structure of 2H-MoS$_2$ after thermal treatment and molecular functionalization, paves the way for a more efficient and effective engineering of both the 2H-MoS$_2$ surface and chemically engineered molecules with specific functionalities that will affect 2H-MoS$_2$ based device performances.

ASSOCIATED CONTENT

Supporting Information.

The following files are available free of charge.

C 1s, O 1s and N 1s core levels of as-received MoS_2 single crystal (Figure S1), and C 1s and O 1s core levels of thiol-functionalized (thermally treated) MoS_2 sample (Figure S2) (PDF)

AUTHOR INFORMATION

Corresponding Authors

*Email: melanie.timpel@unitn.it; marcovittorio.nardi@unitn.it.

Author Contributions

The manuscript was written through contributions of all authors. All authors have given approval to the final version of the manuscript. Δ These authors contributed equally.

ACKNOWLEDGMENT

REFERENCES

(1)   Ganatra, R.; Zhang, Q. Few-Layer MoS_2: A Promising Layered Semiconductor. *ACS Nano* **2014**, *8*, 4074–4099.

(2)   Samadi, M.; Sarikhani, N.; Zirak, M.; Zhang, H.; Zhang, H.-L.; Moshfegh, A. Z. Group 6

Transition Metal Dichalcogenide Nanomaterials: Synthesis, Applications and Future Perspectives. *Nanoscale Horizons* **2018**, *3*, 90–204.

(3)   Wu, W.; Wang, L.; Li, Y.; Zhang, F.; Lin, L.; Niu, S.; Chenet, D.; Zhang, X.; Hao, Y.; Heinz, T. F.; et al. Piezoelectricity of Single-Atomic-Layer MoS2 for Energy Conversion and Piezotronics. *Nature* **2014**, *514*, 470–474.

(4)   Zhou, L.; He, B.; Yang, Y.; He, Y. Facile Approach to Surface Functionalized MoS2 Nanosheets. *RSC Adv.* **2014**, *4*, 32570.

(5)   Nan, H.; Wang, Z.; Wang, W.; Liang, Z.; Lu, Y.; Chen, Q.; He, D.; Tan, P.; Miao, F.; Wang, X.; et al. Strong Photoluminescence Enhancement of MoS2 through Defect Engineering and Oxygen Bonding. *ACS Nano* **2014**, *8*, 5738–5745.

(6)   Makarova, M.; Okawa, Y.; Aono, M. Selective Adsorption of Thiol Molecules at Sulfur Vacancies on MoS2(0001), Followed by Vacancy Repair via S-C Dissociation. *J. Phys. Chem. C* **2012**, *116*, 22411–22416.

(7)   Hong, J.; Hu, Z.; Probert, M.; Li, K.; Lv, D.; Yang, X.; Gu, L.; Mao, N.; Feng, Q.; Xie, L.; et al. Exploring Atomic Defects in Molybdenum Disulphide Monolayers. *Nat. Commun.* **2015**, *6*, 1–8.

(8)   Wu, Z.; Ni, Z. Spectroscopic Investigation of Defects in Two-Dimensional Materials. *Nanophotonics* **2017**, *6*, 1219–1237.

(9)   Wang, S.; Lee, G. Do; Lee, S.; Yoon, E.; Warner, J. H. Detailed Atomic Reconstruction of Extended Line Defects in Monolayer MoS2. *ACS Nano* **2016**, *10*, 5419–5430.

(10)   Kc, S.; Longo, R. C.; Addou, R.; Wallace, R. M.; Cho, K. Impact of Intrinsic Atomic

Defects on the Electronic Structure of MoS2 Monolayers. *Nanotechnology* **2014**, *25*, 375703.

(11) Chen, X.; Berner, N. C.; Backes, C.; Duesberg, G. S.; McDonald, A. R. Functionalization of Two-Dimensional MoS2: On the Reaction between MoS2 and Organic Thiols. *Angew. Chemie - Int. Ed.* **2016**, *55*, 5803–5808.

(12) Kim, J. S.; Yoo, H. W.; Choi, H. O.; Jung, H. T. Tunable Volatile Organic Compounds Sensor by Using Thiolated Ligand Conjugation on MoS2. *Nano Lett.* **2014**, *14*, 5941–5947.

(13) Cho, K.; Min, M.; Kim, T. Y.; Jeong, H.; Pak, J.; Kim, J. K.; Jang, J.; Yun, S. J.; Lee, Y. H.; Hong, W. K.; et al. Electrical and Optical Characterization of MoS2 with Sulfur Vacancy Passivation by Treatment with Alkanethiol Molecules. *ACS Nano* **2015**, *9*, 8044–8053.

(14) Canton-Vitoria, R.; Sayed-Ahmad-Baraza, Y.; Pelaez-Fernandez, M.; Arenal, R.; Bittencourt, C.; Ewels, C. P.; Tagmatarchis, N. Functionalization of MoS2 with 1,2-Dithiolanes: Toward Donor-Acceptor Nanohybrids for Energy Conversion. *npj 2D Mater. Appl.* **2017**, *1*, 13.

(15) Ding, Q.; Czech, K. J.; Zhao, Y.; Zhai, J.; Hamers, R. J.; Wright, J. C.; Jin, S. Basal-Plane Ligand Functionalization on Semiconducting 2H-MoS2 Monolayers. *ACS Appl. Mater. Interfaces* **2017**, *9*, 12734–12742.

(16) Bertolazzi, S.; Bonacchi, S.; Nan, G.; Pershin, A.; Beljonne, D.; Samorì, P. Engineering Chemically Active Defects in Monolayer MoS2 Transistors via Ion-Beam Irradiation and Their Healing via Vapor Deposition of Alkanethiols. *Adv. Mater.* **2017**, *29*, 1606760.

(17)　Li, Q.; Zhao, Y.; Ling, C.; Yuan, S.; Chen, Q.; Wang, J. Towards a Comprehensive Understanding of the Reaction Mechanisms Between Defective MoS2 and Thiol Molecules. *Angew. Chemie Commun.* **2017**, *56*, 10501–10505.

(18)　Nguyen, E. P.; Carey, B. J.; Ou, J. Z.; Van Embden, J.; Gaspera, E. Della; Chrimes, A. F.; Spencer, M. J. S.; Zhuiykov, S.; Kalantar-Zadeh, K.; Daeneke, T. Electronic Tuning of 2D MoS2 through Surface Functionalization. *Adv. Mater.* **2015**, *27*, 6225–6229.

(19)　Zhou, W.; Zou, X.; Najmaei, S.; Liu, Z.; Shi, Y.; Kong, J.; Lou, J.; Ajayan, P. M.; Yakobson, B. I.; Idrobo, J. C. Intrinsic Structural Defects in Monolayer Molybdenum Disulfide. *Nano Lett.* **2013**, *13*, 2615–2622.

(20)　Backes, C.; Berner, N. C.; Chen, X.; Lafargue, P.; LaPlace, P.; Freeley, M.; Duesberg, G. S.; Coleman, J. N.; McDonald, A. R. Functionalization of Liquid-Exfoliated Two-Dimensional 2H-MoS2. *Angew. Chemie - Int. Ed.* **2015**, *54*, 2638–2642.

(21)　Tuxen, A.; Kibsgaard, J.; Gøbel, H.; Lægsgaard, E.; Topsøe, H.; Lauritsen, J. V.; Besenbacher, F. Size Threshold in the Dibenzothiophene Adsorption on MoS2 Nanoclusters. *ACS Nano* **2010**, *4*, 4677–4682.

(22)　Tatti, R.; Timpel, M.; Nardi, M. V.; Fabbri, F.; Rossi, F.; Pasquardini, L.; Chiasera, A.; Aversa, L.; Koshmak, K.; Giglia, A.; et al. Functionalization of SiC/SiOx Nanowires with a Porphyrin Derivative: A Hybrid Nanosystem for X-Ray Induced Singlet Oxygen Generation. *Mol Sys Des Eng* **2017**, *2*, 165–172.

(23)　Kolobov, A. V.; Tominaga, J. *Two-Dimensional Transition-Metal Dichalcogenides*; Springer International Publishing, 2016.

(24) Nardi, M. V; Timpel, M.; Ligorio, G.; Morales, N. Z.; Chiappini, A.; Toccoli, T.; Verucchi, R.; Ceccato, R.; Pasquali, L.; List-kratochvil, E. J. W.; et al. Versatile and Scalable Strategy To Grow Sol − Gel Derived 2H-MoS2 Thin Films with Superior Electronic Properties : A Memristive Case. *ACS Appl. Mater. Interfaces* **2018**, *10*, 34392−34400.

(25) Donarelli, M.; Bisti, F.; Perrozzi, F.; Ottaviano, L. Tunable Sulfur Desorption in Exfoliated MoS2 by Means of Thermal Annealing in Ultra-High Vacuum. *Chem. Phys. Lett.* **2013**, *588*, 198–202.

(26) McDonnell, S.; Addou, R.; Buie, C.; Wallace, R. M.; Hinkle, C. L. Defect-Dominated Doping and Contact Resistance in MoS2. *ACS Nano* **2014**, *8*, 2880–2888.

(27) Santoni, A.; Rondino, F.; Malerba, C.; Valentini, M.; Mittiga, A. Electronic Structure of Ar+ Ion-Sputtered Thin-Film MoS2: A XPS and IPES Study. *Appl. Surf. Sci.* **2017**, *392*, 795–800.

(28) Song, S. H.; Joo, M.; Neumann, M.; Kim, H.; Lee, Y. H. Probing Defect Dynamics in Monolayer MoS2 via Noise Nanospectroscopy. *Nat. Commun.* **2017**, *8*, 2121.

(29) Le, D.; Rawal, T. B.; Rahman, T. S. Single-Layer MoS2 with Sulfur Vacancies: Structure and Catalytic Application. *J. Phys. Chem. C* **2014**, *118*, 5346–5351.

(30) Kunstmann, J.; Wendumu, T. B.; Seifert, G. Localized Defect States in MoS2 Monolayers: Electronic and Optical Properties. *Phys. Status Solidi* **2016**, *8*, 1–20.

(31) Pandey, M.; Rasmussen, F. A.; Kuhar, K.; Olsen, T.; Jacobsen, K. W.; Thygesen, K. S. Defect-Tolerant Monolayer Transition Metal Dichalcogenides. *Nano Lett.* **2016**, *16*, 2234–2239.

(32)   Christodoulou, C.; Giannakopoulos, A.; Nardi, M. V.; Ligorio, G.; Oehzelt, M.; Chen, L.; Pasquali, L.; Timpel, M.; Giglia, A.; Nannarone, S.; et al. Tuning the Work Function of Graphene-on-Quartz with a High Weight Molecular Acceptor. *J. Phys. Chem. C* **2014**, *118*, 4784–4790.

(33)   Christodoulou, C.; Giannakopoulos, A.; Ligorio, G.; Oehzelt, M.; Timpel, M.; Niederhausen, J.; Pasquali, L.; Giglia, A.; Parvez, K.; Müllen, K.; et al. Tuning the Electronic Structure of Graphene by Molecular Dopants: Impact of the Substrate. *ACS Appl. Mater. Interfaces* **2015**, *7*, 19134–19144.

(34)   Lee, S. Y.; Kim, U. J.; Chung, J.; Nam, H.; Jeong, H. Y.; Han, G. H.; Kim, H.; Oh, H. M.; Lee, H.; Kim, H.; et al. Large Work Function Modulation of Monolayer MoS2 by Ambient Gases. *ACS Nano* **2016**, *10*, 6100–6107.

(35)   Hu, C.; Yuan, C.; Hong, A.; Guo, M.; Yu, T.; Luo, X. Work Function Variation of Monolayer MoS2 by Nitrogen-Doping. *Appl. Phys. Lett.* **2018**, *113*, 1–6.

(36)   Li, H.; Paramonov, P.; Brédas, J.-L. Theoretical Study of the Surface Modification of Indium Tin Oxide with Trifluorophenyl Phosphonic Acid Molecules: Impact of Coverage Density and Binding Geometry. *J. Mater. Chem.* **2010**, *20*, 2630–2637.

(37)   Schlesinger, R.; Xu, Y.; Hofmann, O. T.; Winkler, S.; Frisch, J.; Niederhausen, J.; Vollmer, A.; Blumstengel, S.; Henneberger, F.; Rinke, P.; et al. Controlling the Work Function of ZnO and the Energy-Level Alignment at the Interface to Organic Semiconductors with a Molecular Electron Acceptor. *Phys. Rev. B* **2013**, *87*, 155311.

(38)   Hofmann, O. T.; Rinke, P. Band Bending Engineering at Organic/Inorganic Interfaces

Using Organic Self-Assembled Monolayers. *Adv. Electron. Mater.* **2017**, *3*, 1600373.

(39) Addou, R.; Colombo, L.; Wallace, R. M. Surface Defects on Natural MoS2. *ACS Appl. Mater. Interfaces* **2015**, *7*, 11921–11929.

(40) Van Reenen, S.; Kouijzer, S.; Janssen, R. A. J.; Wienk, M. M.; Kemerink, M. Origin of Work Function Modification by Ionic and Amine-Based Interface Layers. *Adv. Mater. Interfaces* **2014**, *1*, 1400189.

(41) Zhong, W.; Chen, L.; Xiao, S.; Huang, L.; Chen, Y. A Versatile Buffer Layer for Polymer Solar Cells: Rendering Surface Potential by Regulating Dipole. *Adv. Funct. Mater.* **2015**, *25*, 3164–3171.

(42) Leung, C.; Kao, L.; Su, S.; Feng, J.; Chan, T. Relationship between Surface Dipole, Work Function and Charge Transfer: Some Exceptions to an Established Rule. *Phys. Rev. B* **2003**, *68*, 195408.

(43) Sim, D. M.; Kim, M.; Yim, S.; Choi, M. J.; Choi, J.; Yoo, S.; Jung, Y. S. Controlled Doping of Vacancy-Containing Few-Layer MoS2 via Highly Stable Thiol-Based Molecular Chemisorption. *ACS Nano* **2015**, *9*, 12115–12123.

(44) Kim, I. S.; Sangwan, V. K.; Jariwala, D.; Wood, J. D.; Park, S.; Chen, K. S.; Shi, F.; Ruiz-Zepeda, F.; Ponce, A.; Jose-Yacaman, M.; et al. Influence of Stoichiometry on the Optical and Electrical Properties of Chemical Vapor Deposition Derived MoS2. *ACS Nano* **2014**, *8*, 10551–10558.

(45) Chen, Y.; Huang, S.; Ji, X.; Adepalli, K.; Yin, K.; Ling, X.; Wang, X.; Xue, J.; Dresselhaus, M.; Kong, J.; et al. Tuning Electronic Structure of Single Layer MoS2 through Defect and

Interface Engineering. *ACS Nano* **2018**, *12*, 2569–2579.

(46) Ponomarev, E.; Pásztor, Á.; Waelchli, A.; Scarfato, A.; Ubrig, N.; Renner, C.; Morpurgo, A. F. Hole Transport in Exfoliated Monolayer MoS2. *ACS Nano* **2018**, *12*, 2669–2676.

(47) Roy, S.; Choi, W.; Jeon, S.; Kim, D.; Kim, H.; Yun, S. J. Atomic Observation of Filling Vacancies in Monolayer Transition Metal Sulfides by Chemically Sourced Sulfur Atoms. *Nano Lett.* **2018**, *18*, 4523–4530.

(48) Gunter, P. L. J.; Niemantsverdriet, J. W. Thickness Determination of Uniform Overlayers on Rough Substrates by Angle-Dependent XPS. **1995**, *89*, 69–76.

(49) Wang, Q.; Ligorio, G.; Diez-Cabanes, V.; Cornil, D.; Kobin, B.; Hildebrandt, J.; Nardi, M. V.; Timpel, M.; Hecht, S.; Cornil, J.; et al. Dynamic Photoswitching of Electron Energy Levels at Hybrid ZnO/Organic Photochromic Molecule Junctions. *Adv. Funct. Mater.* **2018**, *28*, 1800716.

TOC Graphic